

Supplementary Information

Systemic and Tumor-targeted Delivery of siRNA by Cyclic NGR and *isoDGR* Motif-containing Peptides

Yuanyu Huang^{1*}, Qiang Cheng¹, Xingyu Jin⁴, Jia-Li Ji⁴, Shutao Guo², Shuquan Zheng¹,
Xiaoxia Wang¹, Huiqing Cao¹, Shan Gao⁴, Xing-Jie Liang², Quan Du^{1*}, Zicai Liang^{1,3*}

¹ Institute of Molecular Medicine; State Key Laboratory of Natural and Biomimetic Drugs, School of Pharmaceutical Sciences; Peking University, Beijing 100871, China

² Chinese Academy of Sciences Key Laboratory for Biomedical Effects of Nanomaterials and Nanosafety, National Center for Nanoscience and Technology of China, Beijing 100190, China

³ Collaborative Innovation Center of Chemical Science and Engineering (Tianjin), Tianjin 300072, China

⁴ Suzhou Ribo Life Science Co. Ltd., Jiangsu 215300, China

* Correspondence should be addressed to Y. Huang (yyhuang@pku.edu.cn, Tel: +86-10-62750683), Z. Liang (liangz@pku.edu.cn, Tel./fax: +86-10-62769862) or Q. Du (quan.du@pku.edu.cn, Tel./Fax: +86-10-82805780).

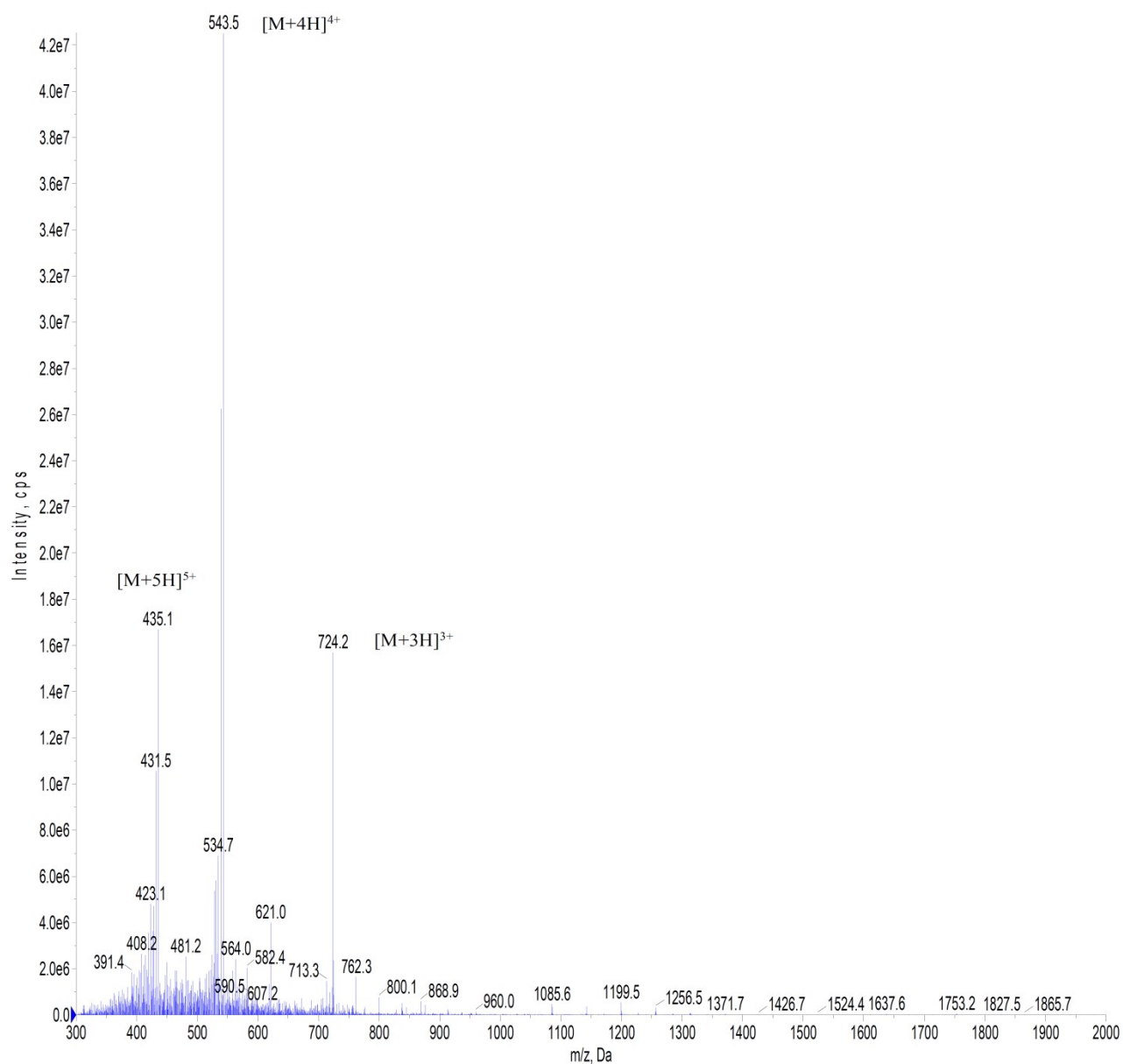
Supplementary figure S1**Mass spectrum of NGR-10R peptide.**

Figure S1. The mass spectrum of NGR-10R peptide.

Supplementary table S1 and figure S2

Receptor expression profile of MDA-MB-231 cell

Although it has been reported that MDA-MB-231 lowly expresses CD13¹⁻³ and highly expresses $\alpha_v\beta_3$ (CD13⁻/ $\alpha_v\beta_3^+$)⁴⁻⁶, it is not uncommon that gene expression levels and profiles vary lab to lab for seemingly identical cell lines. Hence, PCR assay was performed to confirm that the MDA-MB-231 cells used in this study do indeed exhibit the reported CD13/integrin expression profile.

The total RNA of MDA-MB-231 cell was extracted according to a standard protocol. One microgram of total RNA was converted to cDNA using an RNA PCR kit (Takara, Shiga, Japan). Portions of unamplified cDNA were subjected to PCR with a reaction system of 10 μ l of reaction mix (containing Tag enzyme, dNTP, MgCl₂ and reaction buffer, purchase from Beijing CoWin Biotech), 2 μ l of cDNA, 1 μ l of primer set (containing the forward and reverse primers, 5 μ M) and 7 μ l of ddH₂O. This reaction system was first hot-started for 5 min at 95 °C before 35 cycles of 30 s at 95 °C, 30 s at 60 °C and 30 s at 72 °C. The PCR product was loaded into a 1% (w/v) agarose gel and separated for 20 min at a constant voltage of 120 V in 1 \times TAE running buffer. Finally, the gel was analyzed with a UV illuminator (Vtlber Lourmat, France) to show the locations of the PCR products. Two replicates were employed for each PCR reaction in this assay, as indicated with 'a' and 'b' in supplementary figure S2. The PCR primer sets, as shown in supplementary table S1, were selected from literatures to amplify GAPDH, integrin α_v (ITGAV) and CD13, respectively. GAPDH was included as a control of the experimental process.

Table S1. The primer sets used in PCR assay.

Gene	Forward (5'-3')	Reverse (5'-3')	Product length (bp) ^a	T _m (°C)	References
GAPDH	GCTCTCTGCTCCTCC TGTTCC	ACGACCAAATCCGTT GACTC	115	60	7-9
ITGAV	TGTGCAGCCACTACC CATCTCAAT	CGTTCAAACCAGCCA ACCAACA	201	60	10
CD13	ACGCCACCTCTACCA TCATC	AGCACCACCTCCTTG TTCTC	304	60	11

^a: product length is predicted with "Primer-BLAST" tool on NCBI website (<http://www.ncbi.nlm.nih.gov/tools/primer-blast/>).

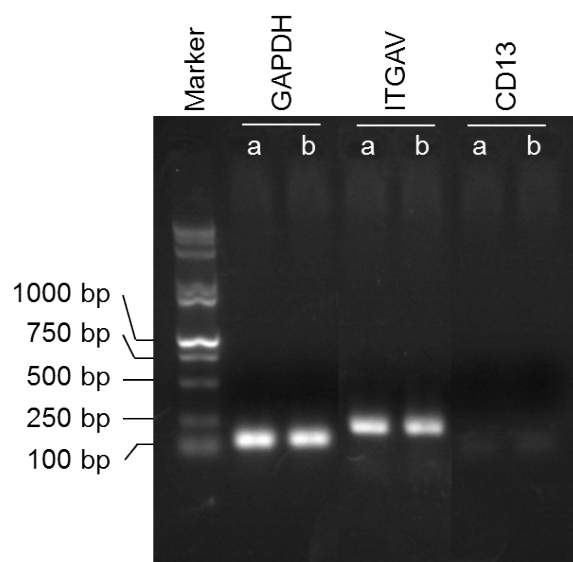


Figure S2 Expression profiles of GAPDH, ITGAV (integrin α_v) and CD13 in MDA-MB-231. This data demonstrated that MDA-MB-231 highly expressed integrin α_v and lowly expressed CD13, in accordance with the profiles reported by literatures¹⁻⁶.

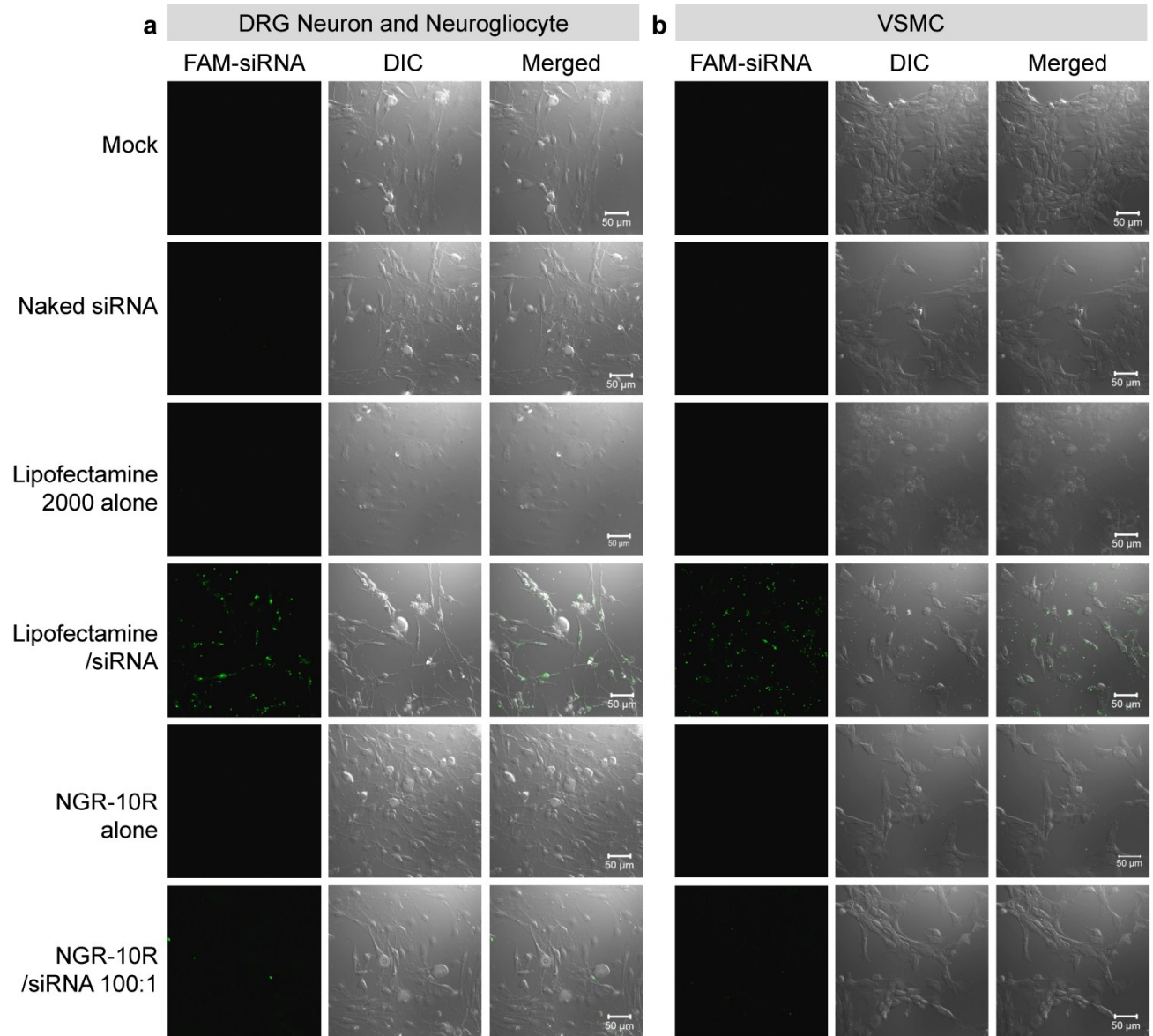
Supplementary figure S3**NGR-10R mediated siRNA transfection into primary DRG neurons, neurogliocytes and VSMCs**

Figure S3 siRNA transfection mediated by NGR-10R peptide in (a) primary rat dorsal root ganglia (DRG) neurons, neurogliocytes and (b) primary vascular smooth muscle cells (VSMCs). Scale bar: 50 µm.

Supplementary figure S4-S5

Subcellular distribution of NGR-10R/siRNA complexes in kidney and submandibular gland

MDA-MB-231 xenografted BALB/c nude mice were employed to explore the tumor targeting properties of NGR-10R/siRNA complexes. When the mice were sacrificed at the end observation time point, kidneys, submandibular gland, heart, liver, lung, as well as tumor tissues, were collected and embedded with OCT in Omnisette tissue cassettes. Then the cryosections of these tissues were prepared according to the same protocol described in the section of '*in vivo* tumor-targeting properties of NGR-10R/siRNA complexes' in the main text. The tumor cryosections recorded with confocal microscope were shown in figure 7d in the main text. Here, cryosections of kidney and submandibular gland were further displayed in figure S4 and S5, respectively. However, the cryosections of heart, liver and lung were not shown, since no fluorescence signal was observed for these three organs, which was in accordance with the imaging data of isolated organs of the tumor-bearing mice (Fig. 7b, c).

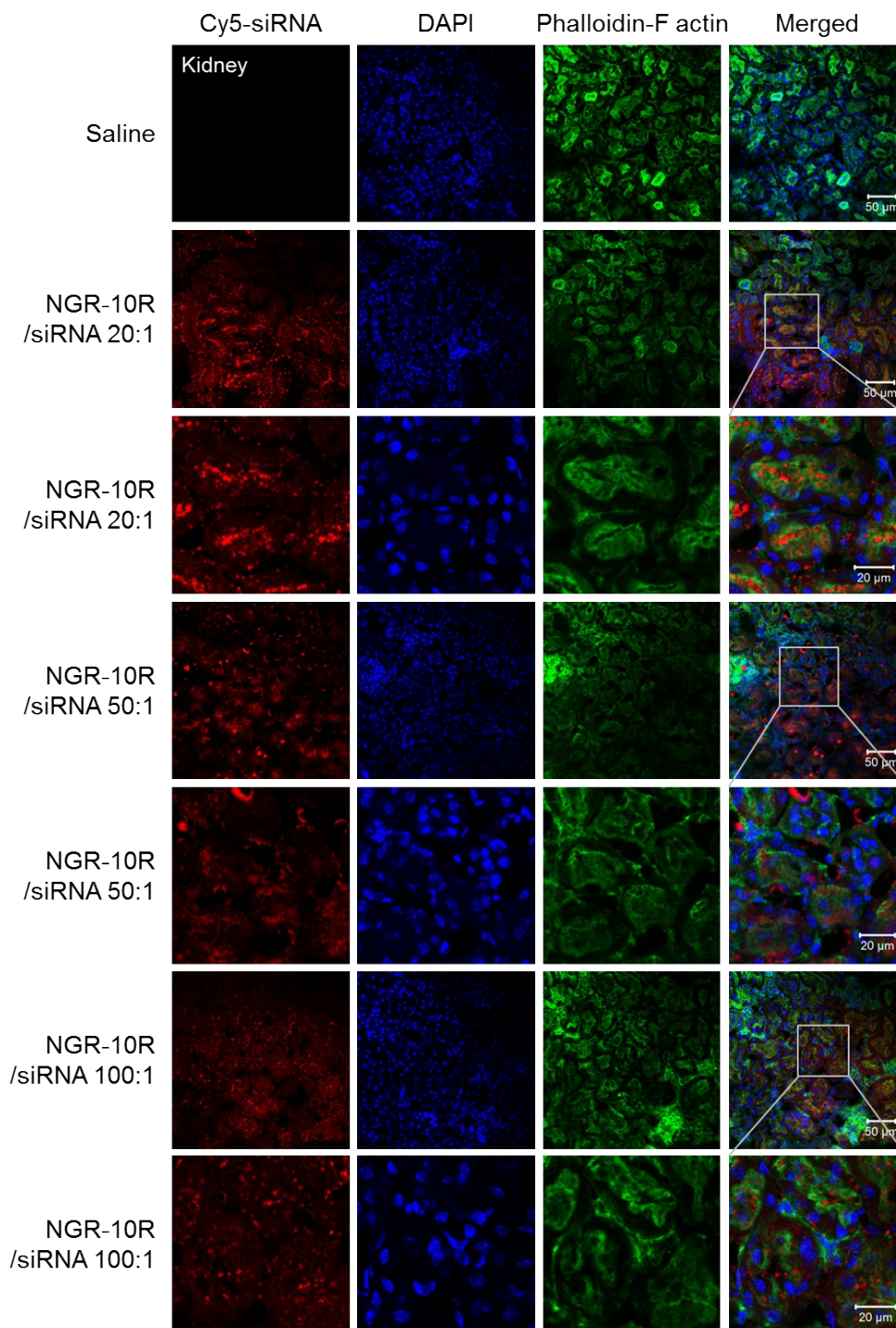


Figure S4 Confocal laser scanning microscopy (CLSM) images of kidney cryosections prepared with tumor-bearing mice. For the complexes of NGR-10R/siRNA with the molar ratios of 20:1, 50:1 and 100:1, magnified images (the lower panels) were acquired by zooming in the indicated areas of their parental images (the upper panels). The scale bars were shown in the lower right corners of the merged images.

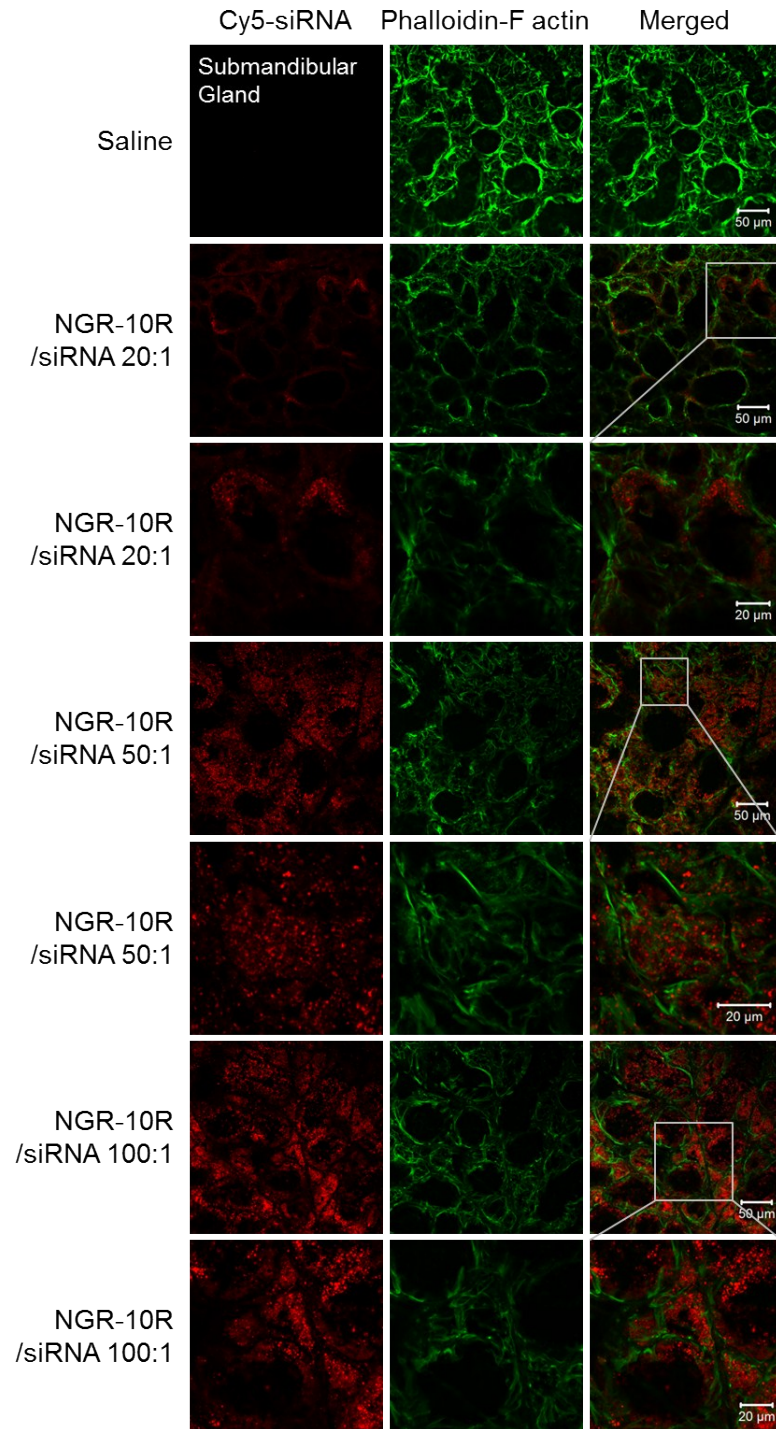


Figure S5 Confocal laser scanning microscopy (CLSM) images of submandibular gland cryosections prepared with tumor-bearing mice. For the complexes of NGR-10R/siRNA with the molar ratio of 20:1, 50:1 and 100:1, magnified images (the lower panels) were acquired by zooming in the indicated areas of their parental images (the upper panels). The scale bars were shown in the lower right corners of the merged images.

Supplementary figure S6

Cytotoxicity of NGR-10R/siRNA complexes

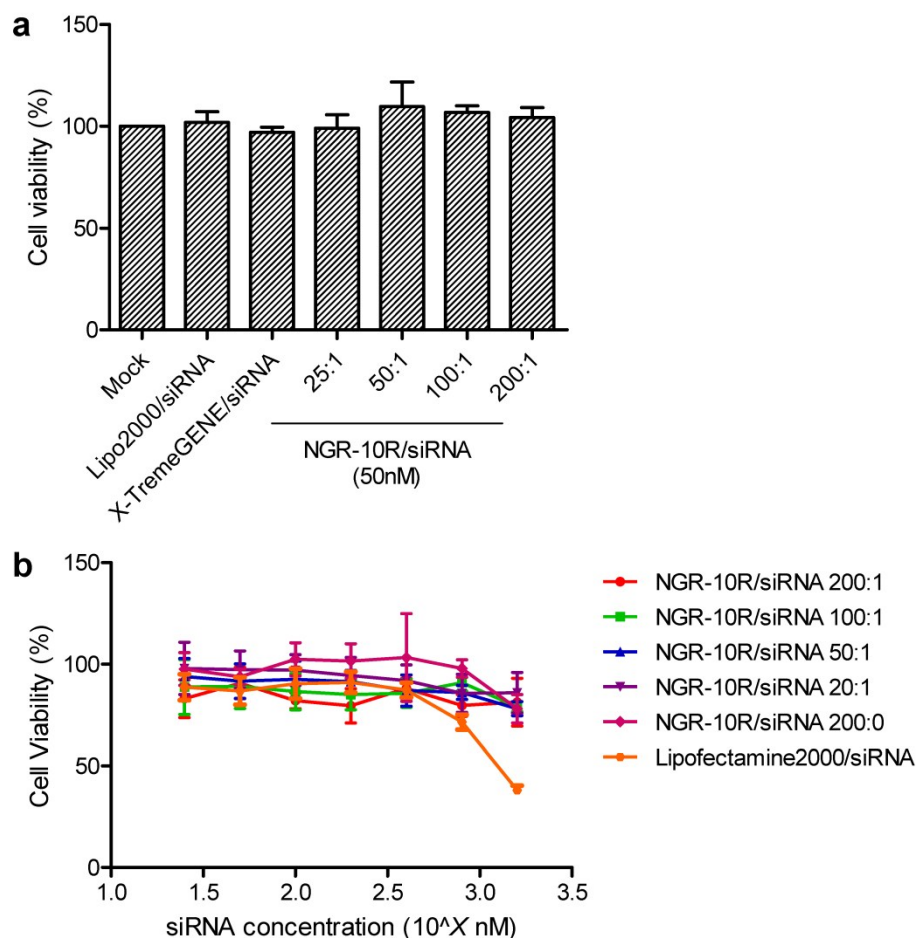


Figure S6 Relative cell viability of MDA-MB-231 cells treated with various formulations. (a) Cell viability of MDA-MB-231 cells transfected with formulations containing 6 pmol siRNA. The corresponding transfection concentration in 96 wells plate was 50 nM. (b) Cell viability of MDA-MB-231 cells after being treated with formulations containing different amounts of siRNA. The transfection concentrations of siRNA ranged from 1600 nM to 25 nM. Here, commercial transfection reagents, lipofectamine 2000 and X-tremeGENE, were employed as controls. In addition, blank NGR-10R without siRNA loading, 'NGR-10R/siRNA 200:0', served as another control by adding equal moles of peptide with 'NGR-10R/siRNA 200:1'.

Supplementary figure S7-S9***In vivo* toxicity of NGR-10R/siRNA complexes in CD-1 mice**

To assess the *in vivo* toxicity of NGR-10R/siRNA formulations, several important parameters were recorded. Six-to-eight week-old CD-1 mice with the weight of 18-22 g were randomly divided into 4 groups. Each experimental group consisted of 6 mice (half male and half female). After randomization, 1×PBS, NGR-10R/siRNA complexes with molar ratios of 20:1 and 50:1 were intravenously injected into the mice. The siRNA dose of peptide/siRNA complexes was 2.5 mg/kg, in accordance with the dosage used in biodistribution and tumor-targeting assays. Lipopolysaccharide (LPS) was intraperitoneally injected into the mice at a dose of 5.0 mg/kg. LPS and PBS were included as positive and negative control, respectively. The body weights of mice were recorded before being sacrificed by cervical dislocation at 4, 24 and 72 hours post administration. The blood was collected, and the weights of liver and spleen were also recorded. Then the serum specimens were harvested by centrifuging the blood samples for 15 min at 3000 rpm at room temperature, followed by diluting three times with 1×PBS before being applied to perform serum biochemistry and cytokine analysis. Then six serum parameters, alanine transaminase (ALT), aspartate transaminase (AST), creatinine (CREA), urea, triglyceride (TG) and total protein (TP), were measured with biochemical analyzer. Meanwhile, three important cytokines, TNF-alpha, IFN-gamma and IL-6, were evaluated with ELISA kit (Beijing 4A Biotech Co.,Ltd., Beijing, China). All detection values of serum-biochemistry parameters and cytokines were directly plotted and shown in supplementary figure S8 and S9 without multiplying them by 3 again.

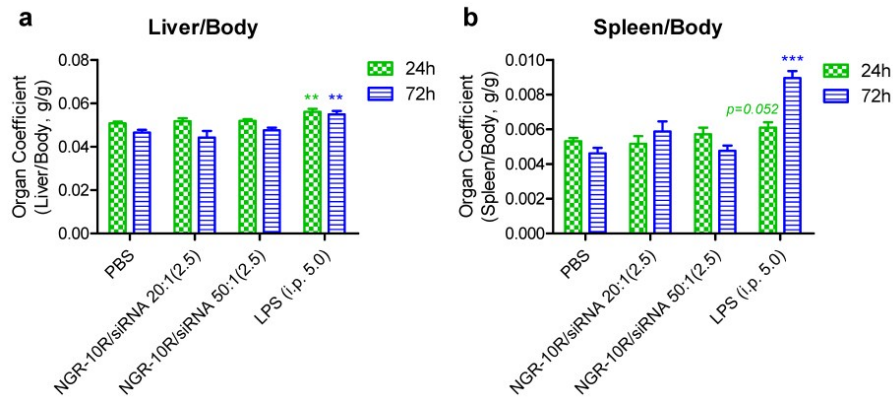


Figure S7 Organ coefficients of mice treated with peptide/siRNA complexes and lipopolysaccharide (LPS). (a) Liver coefficient; (b) spleen coefficient. The data were shown as mean \pm SEM, n = 6. **: $p < 0.01$; ***: $p < 0.001$. vs 1×PBS-treated mice at corresponding time point.

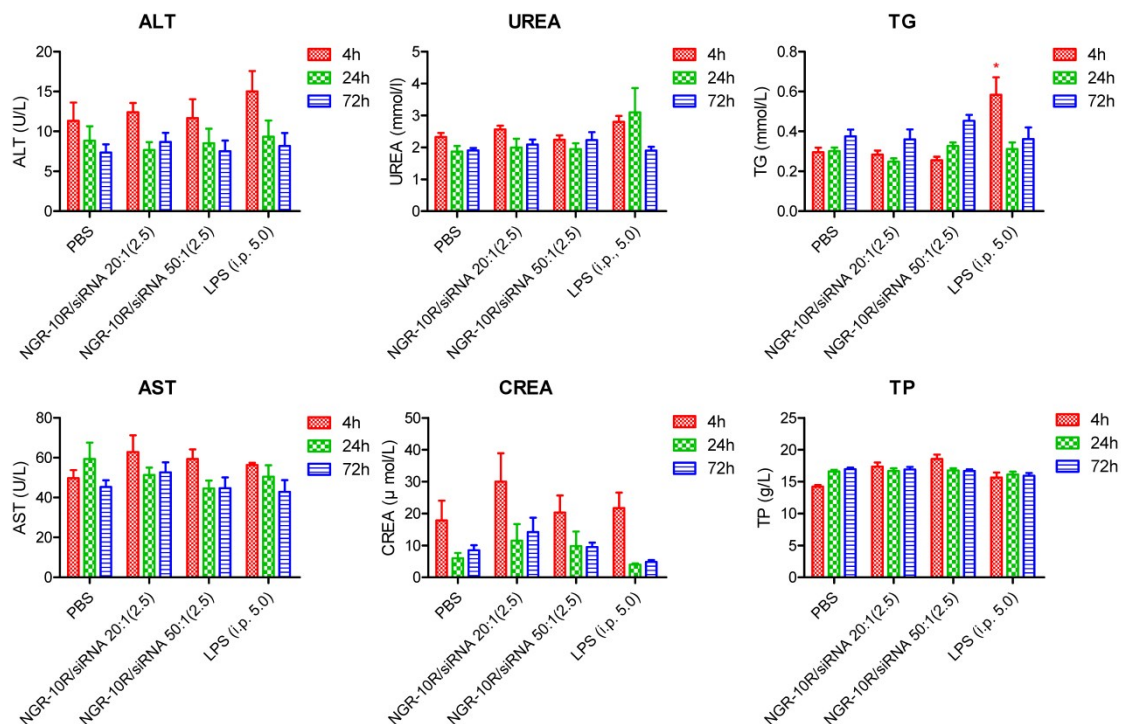


Figure S8 Serum biochemistry of mice treated with various formulations. The samples were diluted three times with 1×PBS before being analyzed with serum biochemistry analyzer. The detection values were directly plotted and shown in figures without multiplying them by 3 again. The data were shown as mean \pm SEM, n = 6. *: $p < 0.05$, vs serum of 1×PBS-treated mice collected at corresponding time point. ALT: alanine transaminase; AST: aspartate transaminase; CREA: creatinine; TG: triglyceride; TP: total protein.

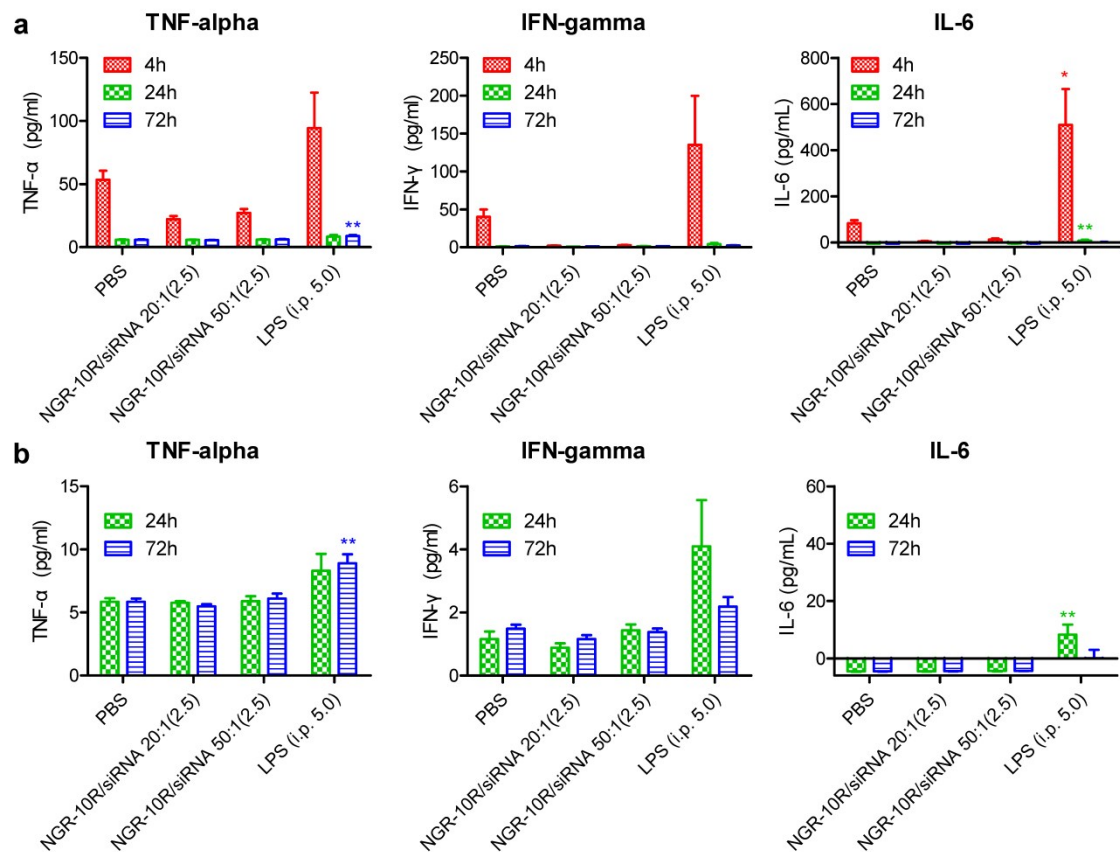


Figure S9 Immunostimulation of peptide/siRNA complexes and LPS. (a) Cytokine level at 4, 24, and 72 hours post injection. (b) Cytokine level at 24, and 72 hours post administration. The samples were diluted three times with 1×PBS before being analyzed with ELISA. The detection values were directly plotted and shown in figures without multiplying them by 3 again. The data were shown as mean ± SEM, n = 6. *: $p < 0.05$, **: $p < 0.01$, vs serum of 1×PBS-treated mice collected at corresponding time point. It seemed that the cytokine level of serum specimens collected at 4 hours, particularly for the group of 1×PBS-treated mice, was somehow different from that of samples collected at the other two time points. However, compared to the corresponding 1×PBS-treated mice at the same time point, no immune activation was observed for peptide/siRNA-treated mice. By contrast, remarkable immunostimulation was found for LPS-treated mice at all three time points post administration since all three cytokines were remarkably elevated.

References

1. L. Hou, X. Zhao, P. Wang, Q. Ning, M. Meng and C. Liu, *PLoS One*, 2013, **8**, e53491.
2. J. S. Shim, J. H. Kim, H. Y. Cho, Y. N. Yum, S. H. Kim, H. J. Park, B. S. Shim, S. H. Choi and H. J. Kwon, *Chem Biol*, 2003, **10**, 695-704.
3. R. Soudy, S. Ahmed and K. Kaur, *ACS Comb Sci*, 2012, **14**, 590-599.
4. S. Takayama, S. Ishii, T. Ikeda, S. Masamura, M. Doi and M. Kitajima, *Anticancer Res*, 2005, **25**, 79-83.
5. Y. Zhao, R. Bachelier, I. Treilleux, P. Pujuguet, O. Peyruchaud, R. Baron, P. Clement-Lacroix and P. Clezardin, *Cancer Res*, 2007, **67**, 5821-5830.
6. P. Wu, X. He, K. Wang, W. Tan, D. Ma, W. Yang and C. He, *J Nanosci Nanotechnol*, 2008, **8**, 2483-2487.
7. H. Seo, I. S. Lee, J. E. Park, S. G. Park, H. Lee do, B. C. Park and S. Cho, *PLoS One*, 2013, **8**, e78776.
8. T. Akagi, N. Hijiya, M. Inomata, N. Shiraishi, M. Moriyama and S. Kitano, *Int J Cancer*, 2012, **131**, 1307-1317.
9. H. J. Choi, T. Y. Kim, S. Ruiz-Llorente, M. J. Jeon, J. M. Han, W. G. Kim, Y. K. Shong and W. B. Kim, *Nucl Med Biol*, 2012, **39**, 1275-1280.
10. T. Choudhuri, S. C. Verma, K. Lan and E. S. Robertson, *Virology*, 2006, **351**, 58-72.
11. A. S. Cowburn, A. Sobolewski, B. J. Reed, J. Deighton, J. Murray, K. A. Cadwallader, J. R. Bradley and E. R. Chilvers, *J Biol Chem*, 2006, **281**, 12458-12467.